LD10

19th International Symposium of Ballistics, 7–11 May 2001, Interlaken, Switzerland

NUMERICAL ANAYSIS OF THE PROPAGATING BLAST WAVE IN A FIRING RANGE

K. Sakamoto[1], K. Matsunaga[2], J. Fukushima[3] and A. Tanaka[4]

[1] Ishikawajima-harima Heavy Industries Co., Ltd., 1, Shin-Nakahara-cho, Isogo-ku, Yokohama, 235-8501, Japan
2 Ishikawajima-harima Heavy Industries Co., Ltd., 2-16, Toyosu 3-chome, Koto-ku, Tokyo, 135-8733, Japan
3 Ishikawajima-harima Heavy Industries Systems Co., Ltd., 2-16, Toyosu 3-chome, Koto-ku, Tokyo, 135-8733, Japan
4 Japan Defense Agency, 2-2-1, Nakumeguro, Meguro-ku, Tokyo, 153-8630, Japan

The objective of this study is to simulate numerically the propagating blast wave in a firing range and to predict the overpressure level. Firing ranges for large cannons are so huge that it is necessary to simplify the problem. The firing range is divided into three domains – A) space near the muzzle device, B) domain around the artillery and C) whole firing range. Computational grids are generated to be paid attention to resolute adequately solid boundaries of the muzzle device, the artillery and the control office in each domain. The solutions on the outer boundaries of each domain are substituted as inner boundary conditions next to other domain. Computational results show the qualitative behavior of blast wave in each domain. The wave shape (N-shape) and the overpressure level of the blast wave show favorable agreement with measured data.

INTRODUCTION

The blast wave propagating in a firing range might damage the hearing organs of operators without some suitable protections. In order to perform firing tests safely in the firing range, it is important to predict the peak overpressure precisely. In this study, a large cannon with complicated muzzle device is focused on without projectile. The computational domain is the whole of the firing range included the artillery and the control office. In order to capture the flow field of the muzzle, high spatial resolution is necessary. On the other hand, the spatial scale of the firing range is much larger than around the muzzle. If the computational grid size of the firing range is as thick as the muzzle device region, big computational memories are necessary. In order to simplify the problem, the firing range is divided into three domains – A) space near the muzzle device, B) domain around the artillery and C) whole firing range (see Fig. 1). Each domain is calculated independently. On the boundaries of each computational domain, physical properties are adopted these solved in correspond to the inner domain. We use personal computer which specifications are as following.

CPU: DEC Alpha 21164A
Clock: 600 MHz
Memory: 320 MB

Thus this simulation can be done within expected the computational memories, time and costs can be saved. This paper describes the useful computational method and typical results on the propagating blast wave in the firing range.

OVERVIEW OF COMPUTATIONAL METHODS

The governing equations are three-dimensional compressible Euler equations. Roe's Flux Difference Splitting[1] is used for the spatial discretization and the high-order accuracy is achieved by the MUSCL interpolation [2,3]. For time integration the 3rd order Runge-Kutta method is used.

The computed domain is divided into three domains – A) space near the muzzle device, B) domain around the artillery and C) whole firing range.

Space near the muzzle device (region A)

The muzzle device of a large cannon is equipped with multi stage baffles. It is a very complicated shape. The exit diameter (D) is selected as reference length. The muzzle device region is treated as two-dimensional model. Figure 2 shows the computational grid (grid = 405 x 123 cells, streamwise direction x direction normal to centerline). The solutions of the circumference direction are approximated with coordinate transformation of the two-dimensional computed results. The grid points near the wall of the muzzle are increased. The solutions of muzzle device region are correspond to the initial condition of this computation in the firing range. At the grid points of the outflow boundary density, temperature, and pressure time histories are recorded. The initial condition of the muzzle device region is assumed to have properties of the propellant gas roughly equivalent to firing tests.

Domain around artillery region (region B)

Figure 3 shows the computational grid around the artillery (grid = 111 x 76 x 60 cells, X x Y x Z). The muzzle region is included in the artillery region. The grid distributions around the artillery are thick and grid points are increased as well as the muzzle device region. The outflow boundary of the muzzle region is corresponded with the inflow boundary of the artillery.

No	θ deg	L/D
M1	0	14
M2	45	13
M3	90	13
M4	135	12

Table 1: Position of pressure

The firing angle is 13 degrees. At the firing tests, four pressure sensors were set up around the artillery and overpressure time histories were measured (see Fig. 4). The pressure sensors were distributed at points on a circle of radius L, angles of theta and height of 10D from the ground (see Table 1). The acquired data of the experiment are compared to the computational results. In this region the outflow boundary density, temperature, and pressure time histories are also recorded for computation of the firing range.

Whole firing range (region C)

Figure 5 shows the computational grid of the firing range (grid=136 x 45 x 51 cells, X x Y x Z). The artillery region is included in the firing range region. The outflow boundary of the artillery region is corresponded with the inflow boundary of the firing range region. The grid points are distributed thickly around the control office.

COMPUTATIONAL RESULTS

Region A

The pressure contour plots at time instants 0.2 and 0.6 msec are shown in Fig. 6. The blast wave passes through the muzzle device. The blast wave flows out and diffuses from each baffle plate. The choked flow and mach disk are well captured between the baffle plates. The computational results show typical flowfields of the muzzle qualitatively.

Region B

Figure 7 shows the pressure contour plots around the artillery at time instants 16.6, 21.7, 30.7 and 35.4 msec. The blast wave generated from the muzzle device region propagates in the artillery region. The blast wave gets over the artillery and flows out from outflow boundary. The propagation of the blast wave to the backward direction takes more time to get over the barrier. The experimental and computational pressure time histories are shown in Fig. 8. These data are recorded at the four measuring points around the artillery above mentioned. It is confirmed that the wave shape (N-shape) and the overpressure level show good agreement with measured data. However it is found that the peak overpressure is truncated. It is necessary to improve further grid refinement.

Region C

Finally, the whole of the firing range is computed. Figure 9 shows pressure contour plots at time instants 33.0 and 89.5 msec. The blast wave generated from the artillery region propagates in the firing range and reaches the control office. The characteristics of the propagating blast wave are captured, tbat is diffusion and spherically development.

However, the truncated solutions in the artillery region are transmitted to the firing region, the blast wave is not clear.

CONCLUDING REMARKS

We tried to compute the propagating blast wave in the whole of firing range considering the characteristics of blast wave. The computational domain is devided into three regions. Computing blast wave of these region seriously, we can simulate by using personal computer in order to compact the computational memory, time and costs. The computational results said the basic characteristics of the propagating blast wave in the firing range can be discussed adequately. That is the direction of the propagating blast wave, the effects of barriers and the comparison with measured data near the artillery. However shape of blast wave were not clear in the position where it is far from muzzle and artillery. In the future, we will refine the spatial resolutions far from muzzle and artillery.

REFERENCES

1. Roe, P.L., "Approximate Riemann Solvers, Parameter Vectors and Difference Schemes", *J. of Computational Physics*, Vol. 43, pp. 357–372, 1981
2. VAN LEER, B., "Towards the Ultimate Conservative Differencing Scheme II: Monotonicity and Conservation Combined in a second order scheme", *J. of Computational Physics*,Vol. 14, pp. 361–370, 1974
3. Fujii, K. and Obayashi, S, "High-Resolution Upwind Scheme for Vortical Flow Simulation", *J. of Aircraft*, Vol. 26, No. 12, 1989

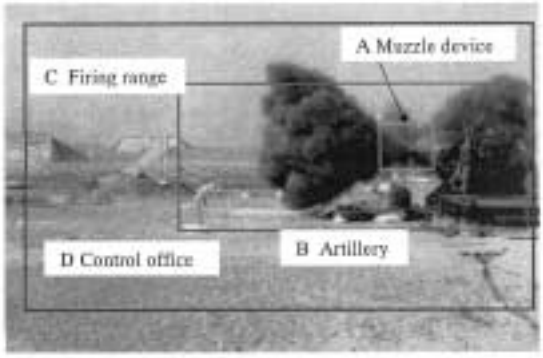

Figure 1: Overview of firing range.

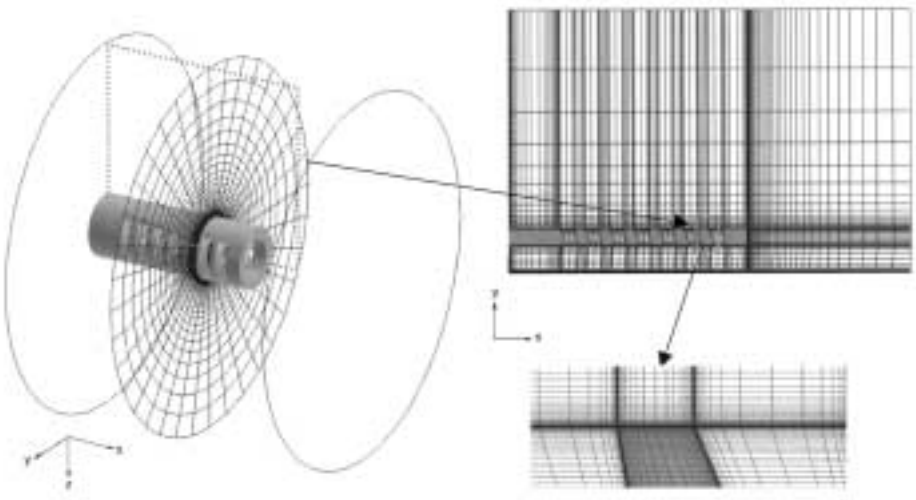

Figure 2: Computational grid of muzzle device (grid = 405 x 123 cells) (region: A).

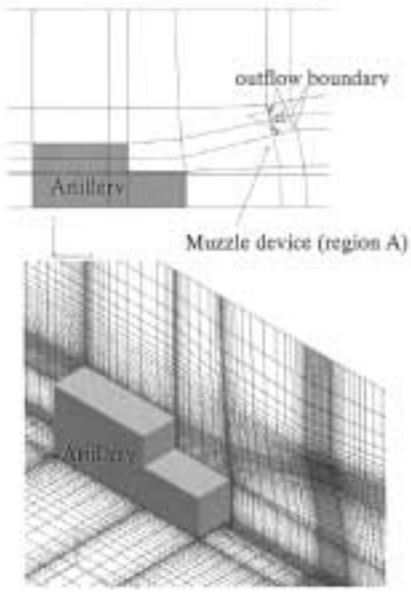

Figure 3: Computational grid around the artillery (region: B) (Grid = 111 x 76 x 60 cells).

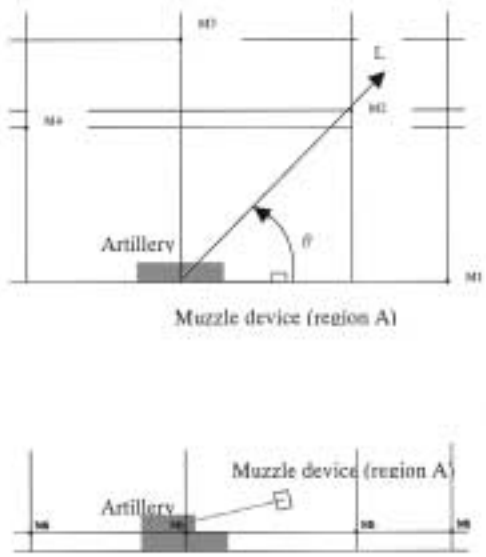

Figure 4: Measurement points (Measurement points = M1, M2, M3, M4).

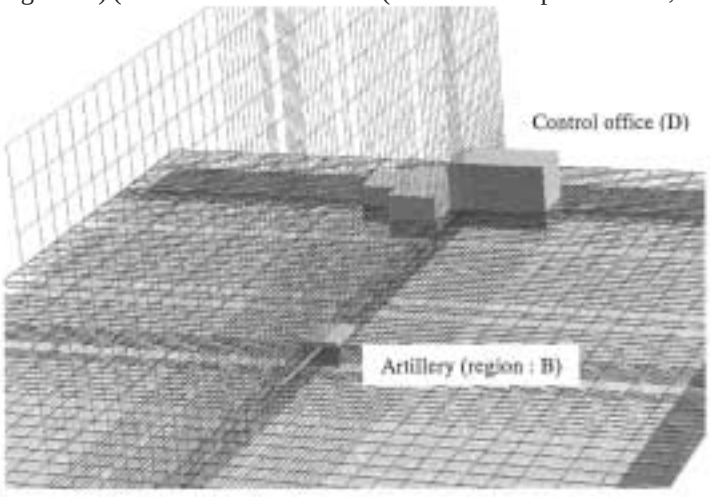

Figure 5: Computational grid of whole firing range (region: C) (Grid = 136 x 45 x 51 cells).

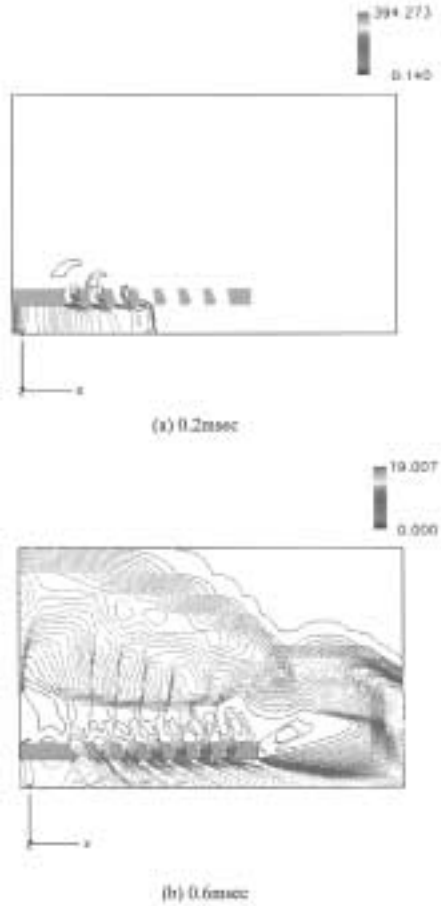

Figure 6: Pressure contour plots of muzzle device region (region: B).

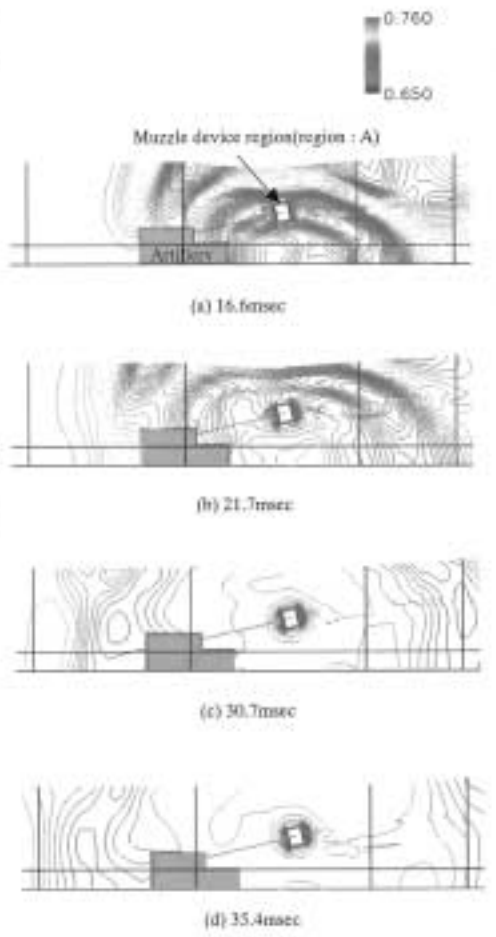

Figure 7: Pressure contour plots of artillery region (region: B).

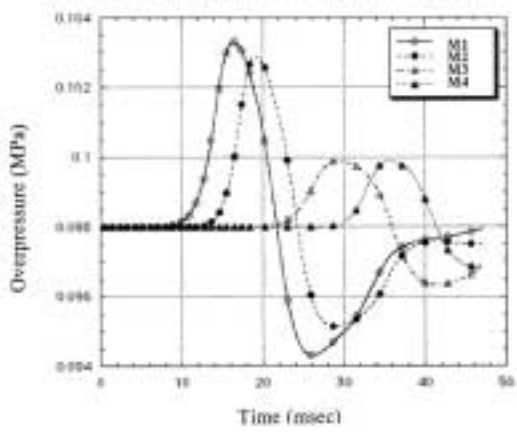

Figure 8: Overpressure time histories at measurement points in the artillery region.

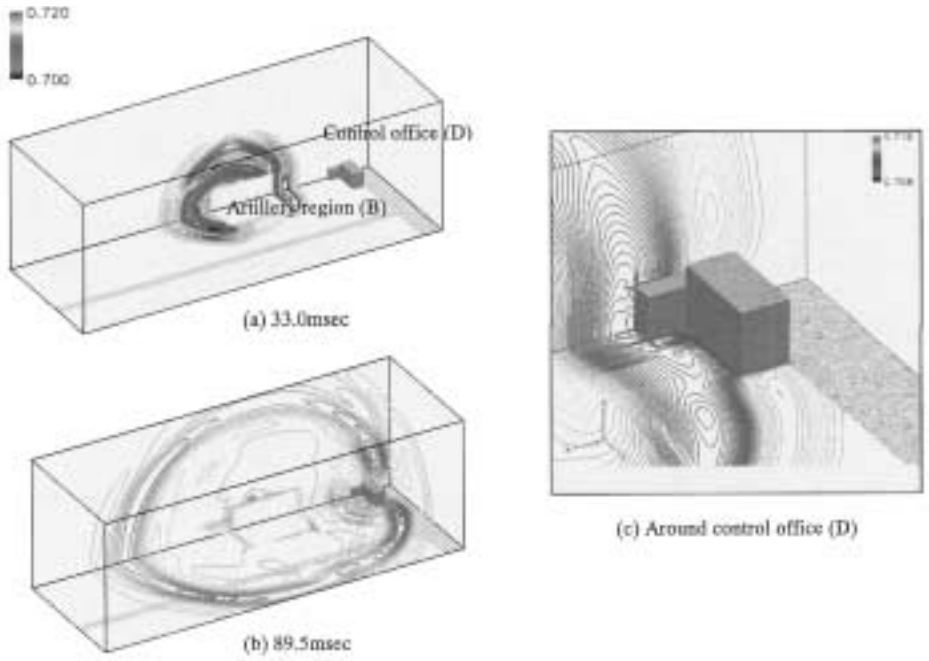

Figure 9: Pressure contour plots of firing range (region: C).